International Research Journal of Engineering and Technology (IRJET) e-ISSN: 2395-0056
Volume: 09 Issue: 08 | Aug 2022 www.irjet.net p-ISSN: 2395-0072

Autonomous Delivery Rocker-Bogie Robot Using Gmapping Based SLAM Algorithm

Magdy Naeem[1], Abdallah Ahmed[1], Fadi Ayman[1], Mohamed Ahmed[1], Ahmed Adel[1], Yehia Amr[1], Mohamed Ashraf[1]

[1]*Mechatronics Engineering Department, Canadian International College, 5th Settlement, Cairo, Egypt*

Abstract - *This paper describes autonomous navigation and its implementation for a non-holonomic autonomous delivery robot using the Robot Operating System (ROS), as well as the robot's full design, implementation, and dynamic modelling. Delivery Based on the rocker and bogie mechanism, the Rocker - Bogie robot aimed to deliver anything from one location to another. The requirement for the development of a highly stable suspension system capable of operating on a variety of terrain surfaces while keeping all wheels in contact with the ground. Adaptive Monte Carlo Localization (AMCL) is used for robot localization, which uses a particle filter to track a robot's pose against a known map. It also makes use of mapping, which is based on the Gmapping package. It is used for laser-based SLAM (Simultaneous Localization and Mapping) mapping. A 2-D occupancy grid map is created using LIDAR. The Dijkstra algorithm is used to plan a path to a goal position using a persistent map created by the robot during the mapping process.*

Key Words: **Autonomous Devilry Robots (ADRs), Robot Operating System (ROS), LIDAR Sensor, SolidWorks, Taguchi method**

1. INTRODUCTION

Mobile robots have been widely used in a variety of tasks, including military and industrial applications, over the last decade.[1–4], planetary exploration [5–8], rescue operations [9,10] as well as home/medical services [11,12]. As a result, it is not surprising that high mobility in a variety of environments has been a primary factor in evaluating the performance of the mobile robot [13]. Mobile robots are classified into three types based on the locomotive mechanism used to achieve the desired mobility: leg-type, track-type, and wheel-type mobile robots. While the leg-type mobile robot has the best adaptability to all environments, its mechanism is quite complicated because active control algorithms with additional actuators and sensors are required to maintain its balance, which inevitably results in slow movement and poor energy efficiency [14,15]. Because of its inherent stability, the track-type mobile robot provides acceptable mobility in an off-road environment, but excessive friction loss during direction change results in poor energy efficiency. [16]. The wheel-type mobile robot is constructed in the simplest configuration compared to other alternatives,, fast movement is guaranteed without any complicated control strategy. However, its adaptability to an environment does not seem to be sufficiently good and its mobility is restricted depending on both the type and the size of encountered obstacle [15,17]. The rocker-bogie design eliminates the need for springs or stub axles in each wheel, allowing the rover to climb over obstacles twice the diameter of the wheel while retaining the rover's manoeuvrabilit.all six wheels on the ground. The tilt stability of any suspension system is limited by the height of the center of gravity. As the weighted side gives, systems with springs tend to tilt more easily. The curiosity rover of the Mars Science Laboratory mission can endure a tilt of at least 45 degrees in either direction without overturning based on its center of gravity, automated sensors prevent the rover from tilting more than 30 degrees [18]. The term “rocker” describes the rocking aspect of the larger links present on each side of the suspension system and the balance of the bogie as these rockers are connected and the vehicle chassis through a modified differential. In the system, “bogie” refers to the conjoining links that have a drive wheel attached at each end. Bogies were commonly used to loading as tracks of army tanks as idlers distributing the load over the terrain. Bogies were also quite commonly used on the trailers of semitrailer trucks as that very time the trucks will have to carry a much heavier load [19]. This robot serves and assists society because it incorporates many engineering fields such as mechanics, electricity, electronics, and design. It also serves hospitals and other public buildings. This thesis delves into the entire process of implementing the proposed prototype, including literature reviews on similar previous robots and control methodologies. The mechanical section of the robot design is then reviewed, which discusses the design and calculations for assembling the rocker-bogie. Then we go to the control section to talk about our control protocol that the robot will use, as well as schematics that show the control sequence for the prototype. NASA has recently launched an ambitious Mars exploration programme. Pathfinder is the first adventurer in this programme. Future rovers will have to travel hundreds of kilometres over months and manipulate rock and soil samples. [20] The first planetary exploration rover was “Lunakhod” which has been sent to Moon2 times with USSR – Luna missions to gather information around the landing site and send pictures of terrain [22]. In 1996, NASA – Jet Propulsion Laboratory and California Institute of Technology have designed new rovers with identical structures named

Sojourner and Marie-Curie. These small rovers were only 10.5 kilograms and the microwave was an oversized Rover Sojourner launched with the Pathfinder landing module in December 1996 [22].

The ADR landscape has been evolving rapidly. In March of 2016, Domino's unveiled what it claimed to be the world's first autonomous pizza delivery vehicle, nicknamed "DRU" or Domino's Robotic Unit. Starship Technologies, founded in 2014, launched its 40-pound delivery robot in March of 2016 in London and partnered with Domino's to deliver pizzas. At the end of April 2018, Starship Technologies announced that it will be rolling out its delivery robot services to corporate and academic campuses in the US and Europe. Starship Technologies has already implemented its delivery services at the Intuit campus in Mountain View, California where average delivery times to customers are less than 15 minutes. In April of 2017, a startup company based in San Francisco called Marble, partnering with Yelp and Eat24, announced that it would be testing its delivery robot. Dispatch, another San Francisco company, announced in April 2016 that it had been working on automatic delivery robots since 2015 and had recently received a $2 million investment to continue to expand the company. In the US market, there are three prominent companies currently developing On-Road Delivery Robots (RADRs). These companies are Nuro, Udelv, and Ford's AutoX. The vehicles each of these companies are prototyping are very different. RADRs are going to be tested in Oklahoma City for supermarket deliveries in early 2019 [23-26].

This article aims to present a rover that can go over extremely rough surfaces such as rocks, bricks, and climbing stairs and avoid any obstacle based on a 360° LIDAR sensor that can draw a live map for the robot. Then we applied robot localization using Adaptive Monte Carlo Localization (AMCL) which uses a particle filter to track the pose of a robot against a known map. It also uses mapping based on the Gmapping package. It provides laser-based SLAM (Simultaneous Localization and Mapping) Gmapping. The LIDAR is used to create a 2-D occupancy grid map. Path planning is established using the Dijkstra algorithm to plan a path to a goal position, using a persistent map created by the robot during the mapping process The conventional suspension system is unable to deal with certain surface conditions, making it difficult to overcome these limits.
The main objective is to design a small autonomous robot using a LIDAR sensor for live mapping to use on road to deliver anything from one location to another, and a highly maneuverable rover robot, it will be designed for working on different platforms like rough terrains, smooth surfaces overcoming obstacles in its path and climbing over obstacles of a certain height, choosing different predetermined gaits and to have good stability, speed as well as payload capacity.

2. SYSTEM DESCRIPTION

In this robot we use aluminum material is used for the base plate because it is rigid and light in weight and steel material for the legs to more stable on road. We use 4 motors on the front and back wheels. On the top of the robot, we put the LIDAR sensor to give a more accurate reading. Motor drives are connected to the 4 DC geared motors which are operated at 12 volts and 100 rpm. The motor driver is controlled by a microcontroller, which provides instructions to the motors according to the commands. The electrical components are powered by two batteries 12V. The wheel diameter chosen is 10cm to satisfy the efficient traveling of the vehicle and it's mostly used as a standard size wheel. This is an autonomous system with no human intervention, which helps the user for more accurate decisions. The flowchart of the robot operations is shown in Figure 2.

Figure 1: Delivery Rocker – Bogie robot Model setup

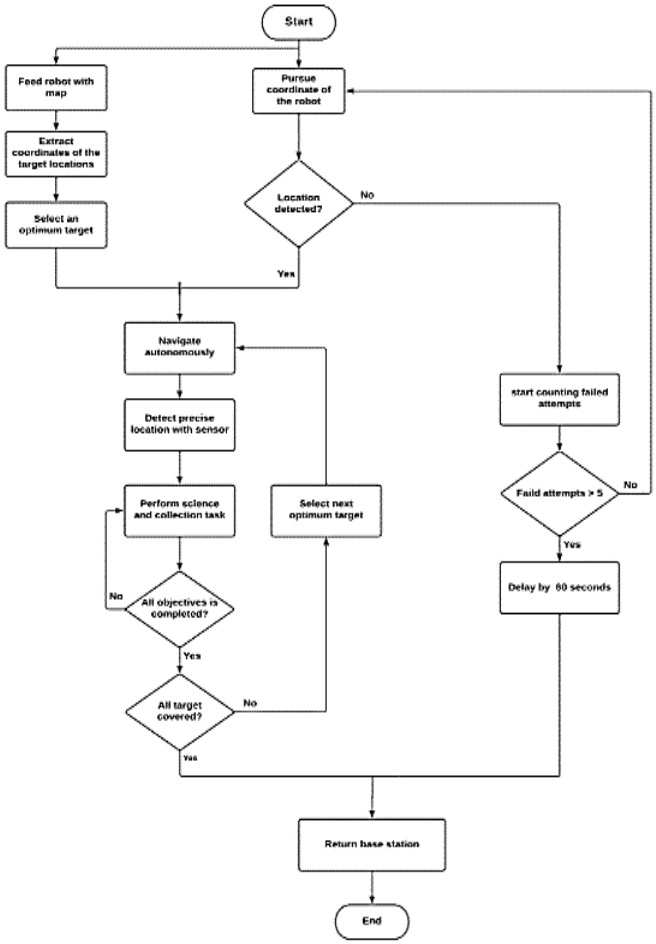

Figure 2: Flow chart diagram

3. TAGUCHI METHODOLOGY

The Taguchi technique is a systematic design methodology that uses the design of experiments or simulations to obtain an optimal value for each parameter. It is quite straightforward and cost-effective not only in establishing the objective function but also in satisfying many quality standards at the same time, as opposed to theoretical optimization approaches that often need complicated mathematical expansions. All key factors affecting performance measures like the signal-to-noise (S/N) ratio can be categorized into two categories using this method: control and noise factors. The control elements are easy to alter to desirable levels since they can be set by a designer, while the noise factors are harder to regulate and may create variances or adverse impacts on product quality. Therefore, such parameters as the wheel radii (R1, R2, and R3) and the link lengths (l1, l2, l3, and l4) are selected as control factors, and three stairs in Fig 3 are selected as noise factors, respectively [28-31].

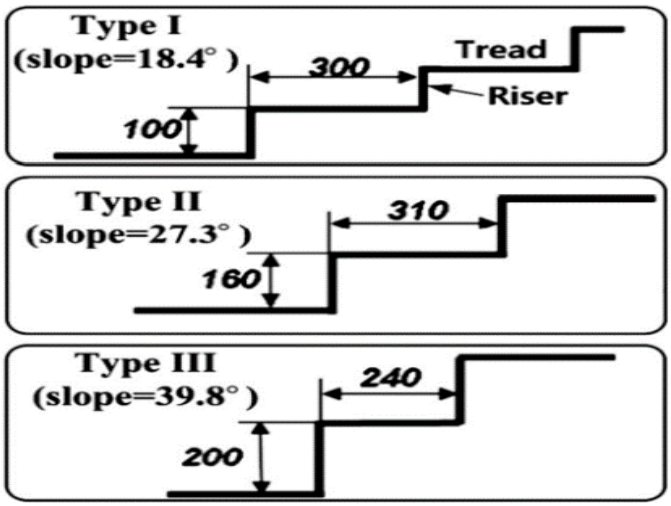

Figure3: Three critical step stars profile

Taguchi methodology was originally developed for quality engineering, and the evaluation and improvement of a product's robustness, tolerance specifications, and quality management of the production process. We optimized the kinematic parameters of a rocker-bogie mechanism as a stair-climbing cart. The optimization was performed using the Taguchi methodology, and the sensitivity analysis results were presented. Constraints were used to determine the initial values of the parameters, and the constraints were checked after choosing the optimal parameters [32-34]. Optimal design is performed in two steps. First, an orthogonal array is used in each optimal design. Then, using sensitivity analysis, the optimal design parameters are determined, and we will show them in tables.

Table 1: Result of each test L18 orthogonal array setup

	Level of the design variable						
Test number	**A l1**	**B l2**	**C l3**	**D l4**	**E r1**	**F r2**	**G r3**
1	1	1	1	1	1	1	1
2	1	2	2	2	2	2	2
3	1	3	3	3	3	3	3
4	2	1	1	2	2	3	3
5	2	2	2	3	3	1	1
6	2	3	3	1	1	2	2
7	3	1	2	1	3	2	3
8	3	2	3	2	1	3	1
9	3	3	1	3	2	1	2
10	1	1	3	3	2	2	1
11	1	2	1	1	3	3	2
12	1	3	2	2	1	1	3
13	2	1	2	3	1	3	2
14	2	2	3	1	2	1	3
15	2	3	1	2	3	2	1
16	3	1	3	2	3	1	2
17	3	2	1	3	1	2	3
18	3	3	2	1	2	3	1

L18 ($2^1 \times 3^7$) orthogonal array is used because it's similar to the parameters that we will use. (J) Determined by experiment according to three kinds of stair structures. We will determine the signal-to-noise ratio (S/N ratio) from that equation 1.

$$S/N = -10Log\left(\frac{1}{n}\sum_1^n ri^2\right) \quad (1)$$

Table 2: Objective function for each stair shape

The objective function for each stair shape			
J1: 300x100	J2: 310x160	J3: 240x200	S/N ratio (dB)
0.2376	0.4179	0.7515	5.762
0.2935	0.3757	0.5866	7.201
0.2457	0.4389	0.6909	6.135
0.2936	0.3742	0.5817	7.253
0.2639	0.4774	0.7694	5.279
0.2356	0.3858	0.7217	6.166
0.1987	0.4432	0.789	5.434
0.2932	0.4072	0.6348	6.61
0.2632	0.4718	0.7538	5.425
0.2545	0.4526	0.7156	5.841
0.1979	0.4096	0.7294	6.084
0.2927	0.4105	0.6512	6.457
0.2514	0.4422	0.6843	6.115
0.2125	0.442	0.774	5.531
0.2992	0.351	0.5431	7.715
0.324	0.3624	0.5924	7.083
0.258	0.4562	0.7131	5.832
0.209	0.3865	0.7295	6.166

The mean is determined to know the effect of the parameters on the response according to equation 2.

$$\text{Mean} = \frac{\sum J}{N} \quad (2)$$

Table 3: Mean values of the 18 Test numbers.

Test number	Mean
1	**0.469**
2	**0.4186**
3	**0.4585**
4	**0.4165**
5	**0.5036**
6	**0.4477**
7	**0.477**
8	**0.4451**
9	**0.4962**
10	**0.4742**
11	**0.4456**
12	**0.4514**
13	**0.4593**
14	**0.4761**
15	**0.3977**
16	**0.4262**
17	**0.4757**
18	**0.4416**

Tables show the Mean of 18 Test numbers, so we need to determine Mean Total. The mean total is equal to the Sum Means of 18 test numbers, Mean total is equal to 8.18. The sum of squares is a measure of the deviation of the experimental data from the mean value of the data. Summing each squared deviation emphasizes the total deviation- square sum (SS) can be calculated according to equation 3.

$$A = \frac{A1^2}{3} + \frac{A2^2}{3} + \frac{A3^2}{3} - \frac{TM^2}{18} \quad (3)$$

Table 4: Sum of Square (SS)

Test number	1	2	3	Sum square (ss)
A	2.7173	2.7009	2.7618	3.7181
B	2.7222	2.7647	2.6931	3.72821
C	2.7007	2.7515	2.7278	3.71778
D	2.7571	2.5555	2.8675	3.73318
E	2.7482	2.7232	2.7086	3.71762
F	2.8225	2.6909	2.6666	3.72204
G	2.7312	2.6936	2.7552	3.71799

There is a standard statistical technique called analysis of variance (ANOVA) that is routinely used to provide a measure of confidence. The technique does not analyse the data directly, but rather determines its variability (variance). The variance is used to calculate confidence. The variance of controllable and noise factors is provided by the analysis. Robust operating conditions can be predicted by understanding the source and magnitude of variance. This is the methodology's second advantage [35]. DOF is a crucial and valuable concept that is difficult to define. It is a measure of how much information can be determined uniquely from a given set of data. The DOF for data about a factor is one less than the number of levels. The experiment can also benefit from the concept of DOF. The concept of DOF can also be extended to the experiment. An experiment with n trials and r repetitions of each trial has n × r trial runs. The total DOF becomes [35]. Variance measures the distribution of the data about the mean of the data. Because the data are representative of only a part of all possible data, DOF rather than the number of observations is used in the calculation [35].

$$\text{Variance} = \frac{Sum\ of\ squares}{Degrees\ of\ freedom} \quad (4)$$

Table 5: ANOVA table

Source	SS	DOF	Var.	F(calc.)
A	3.718	2	1.859	4.2762
B	3.7184	2	1.859105	4.27669
C	3.71778	2	1.85889	4.2757
D	3.73318	2	1.86659	4.3111
E	3.71762	2	1.85881	4.2753
F	3.72204	2	1.86102	4.2855
G	3.71799	2	1.85899	4.27617
Error	4.84898	3	1.61633	
Total	30.8938	17		

3.1 Taguchi Results

- At a 90% confidence level, all of the parameters are statistically significant F2,3at 90% =3.14
- At 95% confidence level parameter D is stat significant F2,3 at 95%=4.302
- At 99% confidence level none of the parameters is stat significant F2,3 at 99%= 9.55
- From signal to noise ratio analysis trial 5 has the best setting
- From ANOVA analysis, we find that the optimal design in trial 5 is our design.

4. COMPONENT DESCRIPTION

A geared DC motor (Here) with 63 RPM and 12 V is used. The rated torque is 28.5 kg-cm. This motor is used to satisfy the need off moving the whole vehicle. Since a lot of weight should be carried, we use this type of motor. Six motors are used here and are controlled with help of a motor driver and a microcontroller. The motors are powered by a 12V battery. The wheel diameter used here is 20cm. There are six wheels used here. These wheels are sufficient to travel on all types of roads. With the rocker bogie mechanism and the design of the wheel, the vehicle can move efficiently through the roads. The base plate of the robot is aluminum because it is rigid and light in weight, but the legs of the robot from steel because it is heavy and rigid to more stability on roads. Two 12V 7.2Ah batteries are used to power the four motors and the microcontroller. This battery is efficient and rechargeable. The microcontroller is can be powered by the same battery by controlling the voltage passing through the controller board. A battery is used because it is portable, Therefore the vehicle need not be powered with wires attached using the electricity through household lines. A type of microcontroller board that is built using Raspberry pi 4B – 8GB microchip and Arduino Mega based on ATmega2560. Arduino is an open-source platform for prototyping, and its simplicity makes it suitable for both hobbyists and professionals to use. There are 54 digital input/output pins on the Arduino Mega (of which 14 can be used as PWM outputs), an ICSP header, a 16 MHz crystal oscillator, a reset button, a power jack, 16 Analog inputs, and a USB interface. This microcontroller board contains enough analog and digital ports which can be used to interface the motors and sensors that are used in the machine Here RPLIDAR A1 is based on the laser triangulation ranging principle and uses high-speed vision acquisition and processing, the system measures distance data more than 8000 times per second. The core of RPLIDAR A1 runs clockwise to perform a 360-degree omnidirectional laser range scanning for its surrounding environment and then generate an outline map for the environment [27].

5. MECHANICAL DESIGN

With the basic assumptions, the Rocker Bogie mechanism calculations are made The Construction and Constraints of Rocker Bogie Mechanism Angle ABC and ADE is equal to 90°, From the Isosceles Triangle formed, Constraints obtained are AC is equal to CE, AD is equal to DE, angle DAE is equal to angle DEA equal to 45°, and Angle ADE is equal to 90°. To ensure the stability of climbing obstacles, the position of one pair of wheels at a time must be raised. So, at first, we find Bogie links dimension.

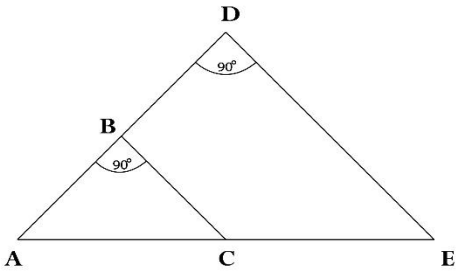

Figure 4 Isosceles Triangle

5.1 Bogie link calculation

We make the setup for calculation as the first pair of wheels placed horizontally at the end of rising with 50mm extra space for safety purposes. on the same second pair is just before the start of raising with 50mm extra space for safety purposes.

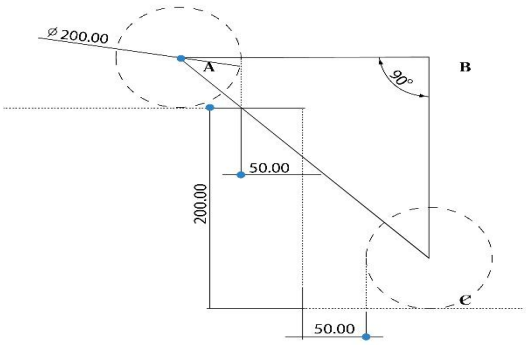

Figure 5 Illustration of wheel Base - Bogie

AB is equal to the sum of the Radius of wheel A, Safety Space A, Safety Space C, and Radius of wheel C. AB is equal to 300 mm, and BC is equal to 150 mm. By Using Pythagoras Theorem in Triangle ABC

$$AC^2 = AB^2 + BC^2 \quad (5)$$

By the Calculations made, the Primary Length of the Bogie link should be of Minimal length 150mm and a wheelbase of 335.4 mm, by considering the manufacturing complexity of the material the following Link length is taken for

further process, AB and BC will be equal 360 mm, AC will be equal to 509.12 mm.

5.2 Rocker link calculation

With the help of values obtained in Bogie links and constraints developed. We construct the Rocker Link. CE is equal to 509.12 mm, AE is the sum of AC and CE, and AE is equal to 1018.23mm, by using Trigonometric Equations: DE is equal to 720mm.

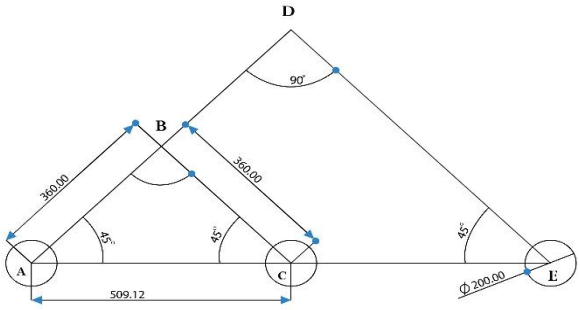

Figure 6 Rocker Bogie Relation Sketch

5.3 Calculating the height of the Triangle ABC and ADE

The top surface of the Rocker Bogie is needed to be flat to fit the box, motor, and battery. So, we cut the top edge of the Triangle ABC such that the height of the Triangle ABC is greater than the Cut edge height from the base. To find the length of the XY bisects line, we form a Triangle DXY. The length of h is equal to 254.56 mm.

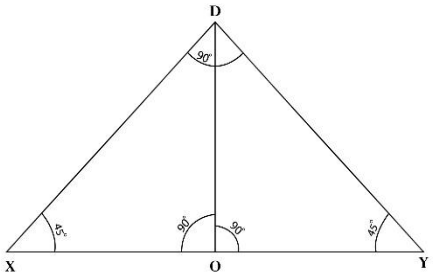

Figure 7 Bisect line of triangle DXY

The length of DO is equal to the difference between the height of triangle ADE and the bisect height from the base, DO is equal to 148.49 mm. Using Trigonometric Equations, XO is equal to 148 49 mm, OY is equal to 148.49mm. Therefore, XY is equal to 300 mm. By all the Calculations and Data obtained, we construct the Rocker Bogie Links dimensions.

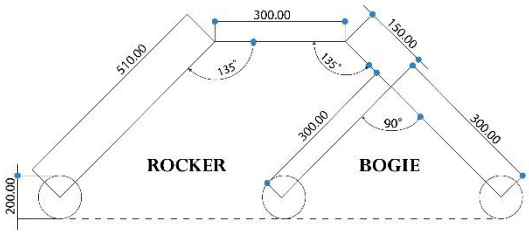

Figure 8 Dimensions of rocker bogie links

5.4 Robot actuators

The required values for proceeding with the calculation are listed below. The values that are mentioned below are standard values and the remaining values are taken from the above calculation.

Table 6: Parameters of the system

Parameters	Values
Nominal bot speed (V)	0.5 m/s
Maximum slope incline (k)	15%
Total robot weight (m)	30kg
Diameter of the wheel (Dw)	0.2m
Co-efficient of drag (Cd)	0.6
Density of air (p)	1.226 kg /m3
Co-efficient of rolling resistance (Crr)	0.01
Frontal Area (A)	0 .158 m2
Efficiency of motor	88%

When considering, the forces acting on the telepresence, the consideration of opposing forces that it has to overcome are taken into account. They are grade resistance, Drag resistance, and rolling resistance. Thrust Force (Ft) is equal to the sum of the grade resistance, Drag resistance, and rolling resistance. Grade resistance is given as the product of the weight and the sine of the angle of inclination. Grade resistance is equal to 44.145 N. Drag force is the force that the vehicle has to move forward. This force increases with increasing speed. The Drag resistance is equal to 0.01452N according to equation 6.

$$\text{Drag resistance} = \frac{\rho A V^2 C_d}{2} \quad (6)$$

$$\text{Rolling resistance} = \text{Mass} * g * Crr \quad (7)$$

The Rolling resistance is equal to 2.943N. The total force (F_t) is equal to the sum of the Grade resistance, Drag resistance, and Rolling resistance. The total force (F_t) is equal to 47.1 N. Torque for traction wheel, per one wheel motor 2.355 Nm. According to the standard dimensions available in the market, we select a motor of torque 28.5kg-cm available. We find the wheel rotation speed

value to evaluate the rpm of the motor. The nominal speed of the robot can be calculated according to equation 8.

$$N = \frac{60 * V}{n * D_w} \quad (8)$$

where D_w is the diameter of the wheel, The nominal speed of the robot is 50 RPM. According to the standard dimensions available in the market, we select a 63 rpm motor.

6. SOLIDWORK MODEL AND FINITE ELEMENT ANALYSIS (FEA)

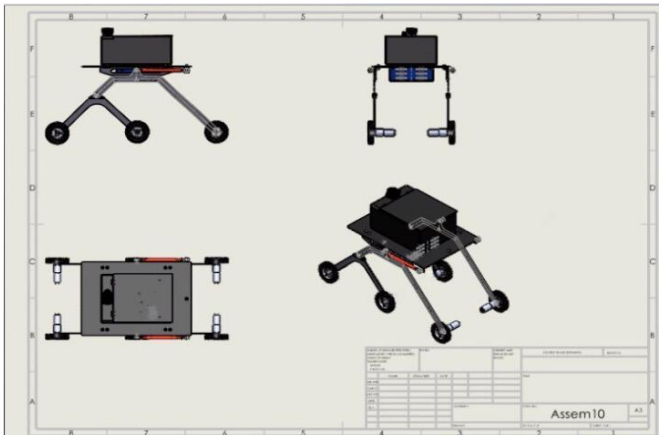

Figure 9 Drawing Sheet

Figure 10 Isometric view in *SolidWorks*

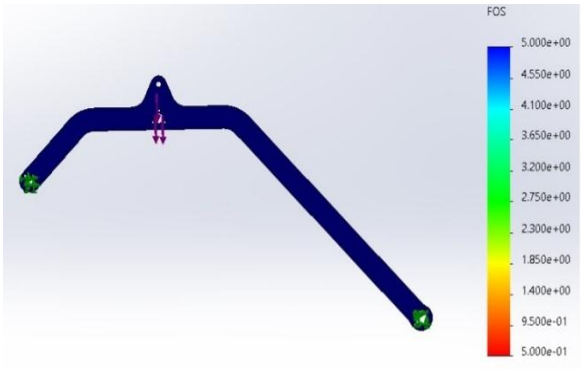

Figure 11 Rocker strain analysis

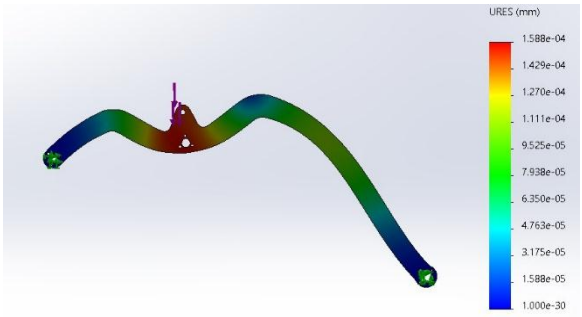

Figure 12 Rocker stress analysis

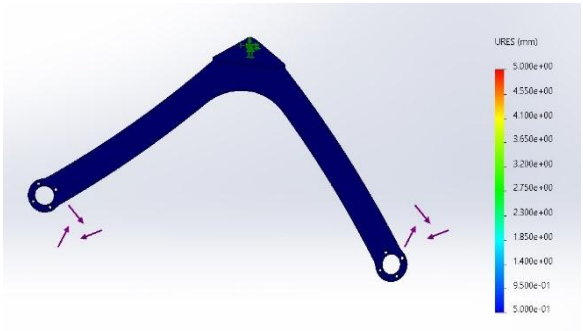

Figure 13 FOS OF Rocker

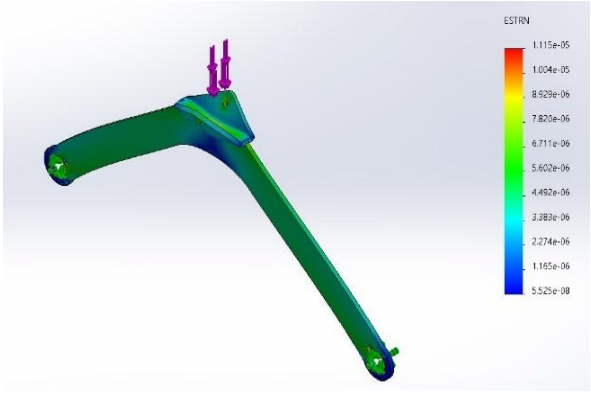

Figure *14* Bogie *Stress* analysis

7. ROS METHODOLOGY

7.1 Kinematic model

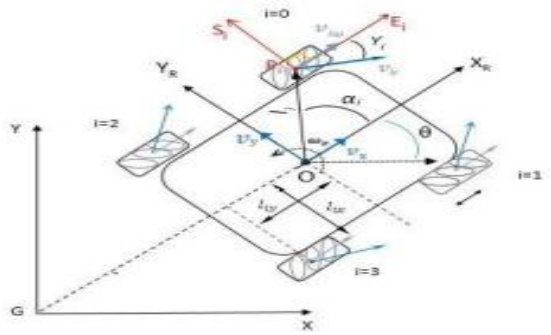

Figure 15 Wheels Configuration and Posture definition

The configuration parameters and system velocities are defined as follows: x, y, θ, robot's position (x, y) and its orientation angle θ (The angle between X and XR); X G Y, inertial frame; x,y are the coordinates of the reference point O in the inertial basis; Xr OYr, robot's base frame; Cartesian coordinate system associated with the movement of the body center; Si Pi Ei, the coordinate system of ith wheel in the wheel's center point Pi ; O, Pi , the inertial basis of the Robot in Robot's frame and Pi = {XPi , YPi } the center of the rotation axis of the wheel i ; OPi , is a vector that indicates the distance between the Robot's center and the center of the wheel ith; lix , liy , lix , half of the distance between front wheels and liy half of the distance between the front wheel and the rear wheels. li , the distance between wheels and the base (center of the robot O); ri , denotes the radius of the wheel i (Distance of the wheel's center to the roller center) rr , denotes the radius of the rollers on the wheels. αi , the angle between OPi and XR ; βi , the angle between S i and XR ; γi , the angle between vir and Ei ; ωi [rad/s], wheels angular velocity; $vi\omega$ $[m/s]$, i = 0,1,2,3 ∈ R , is the velocity vector corresponding to wheel revolutions •vir , the velocity of the passive roller in the wheel i; [wsi wEi ωi] T , Generalized velocity of point Pi in the frame $SiPiEi$; [vSi vEi ωi] T , Generalized velocity of point Pi in the frame $XROYR$; vx , vy [m/s] - Robot linear velocity; ωz [rad/s] - Robot angular velocity;

According to equations for Forward and Inverse kinematics there is:

$$\omega 1 = 1/r\ (vx - vy - (lx + ly)\ \omega),$$

$$\omega 2 = 1/r\ (vx + vy + (\ lx + ly)\ \omega)\ ,$$

$$\omega 3 = 1/r\ (vx + vy - (\ lx + ly)\ \omega\ ),$$

$$\omega 4 = 1\ /r\ (vx - vy + (lx + ly)\ \omega).$$

Longitudinal Velocity:

$$vx(t) = (\omega 1 + \omega 2 + \omega 3 + \omega 4)\ .\ r/4 \qquad (9)$$

Transversal Velocity:

$$vy\ (t) = (-\omega 1 + \omega 2 + \omega 3 - \omega 4).\ r/4 \qquad (10)$$

Angular velocity:

$$\omega z\ (t) = (-\omega 1 + \omega 2 - \omega 3 + \omega 4)\ .\ r/\ 4\ (lx+ly) \qquad (11)$$

The resultant velocity and its direction in the stationery coordinate axis (x, y, z) can be achieved by the following equations

$$V\boldsymbol{R} = \sqrt{vx^2 + vy^2} \qquad (12)$$

7.2 ROS Implementation

In ROS implementation a laptop machine Lenovo-Legon 7i slim [Intel(R) Core (TM) i7-11750HQ CPU @ 4GHz] With 16GB Ram and works as a master computer operated with Linux (Ubuntu) version 18.04 operating system. There is a slave machine that works with the master machine which is Raspberry Pi 4B running Ubuntu-mate 18.04 [36].

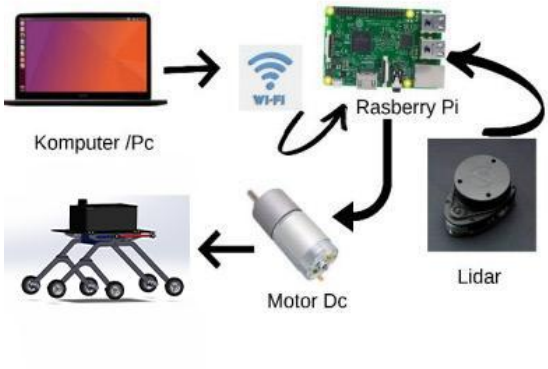

Figure 16 System architecture block diagram of the autonomous

The robot operating system (ROS) is Linux-based, it is a flexible framework for creating robot software. it consists of tools, libraries, and protocols that aim to simplify and create complex robot behavior across numerous robotics platforms [36]. ROS structure consists of packages and nodes that are used to build a complete workspace for the robot, to build the strategy that is followed to build a robot in ROS is to create Nodes to connect to the controller to the ROS environment, while the components, mapping, localization and move_ base nodes are implemented by C++ and python shared libraries that get linked to the node at compiling time.

ROS structure allows the tracked robot to link and synchronize messages between nodes in the master machine and with Raspberry-pi 4 board on board client computer and micro-controller in the robot by the network using roscore

master computer. The nodes contact each other according to topics and are collected and described through the ROS graph diagram as shown in figure 17. It displays several nodes and topics to control tracked robot autonomous systems. Graph of ROS nodes came in the shape of (ellipses) and topics (squares) of the proposed tracked vehicle. The continuous line arrows are topic subscriptions, that moved from the subscriber node to publish it into another node with directions going from the subscriber node to the publisher one.

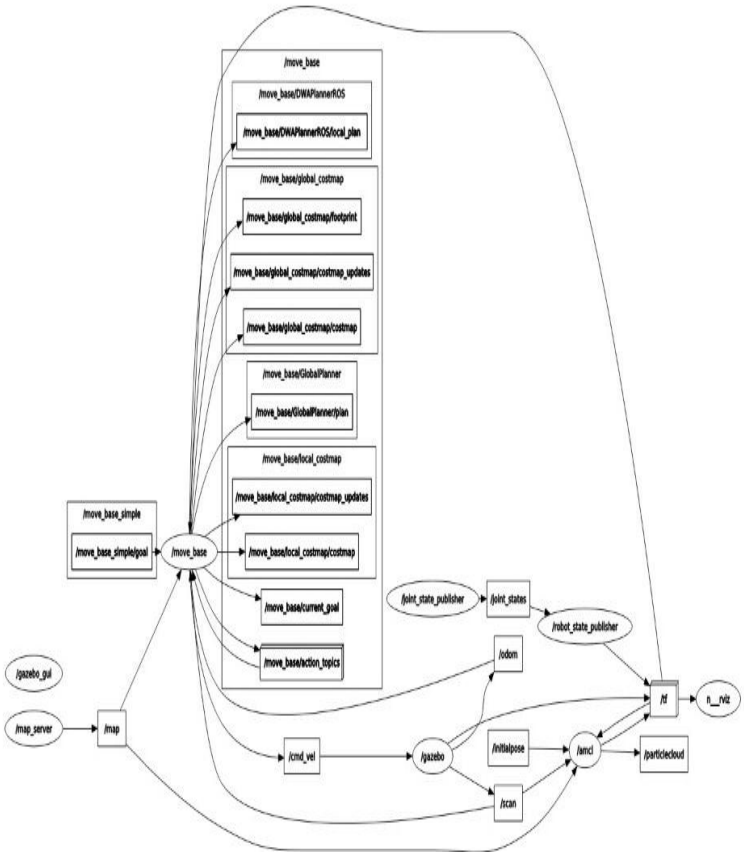

Figure 17 ROS Computation graph diagram rqt graph

For links and joints of the tracked robot autonomous system, it is created by Unified Robot Description format URDF that described in ROS transformation tree frames diagram It shows all the frames involved in the architecture of the system, that shown in figure 18.

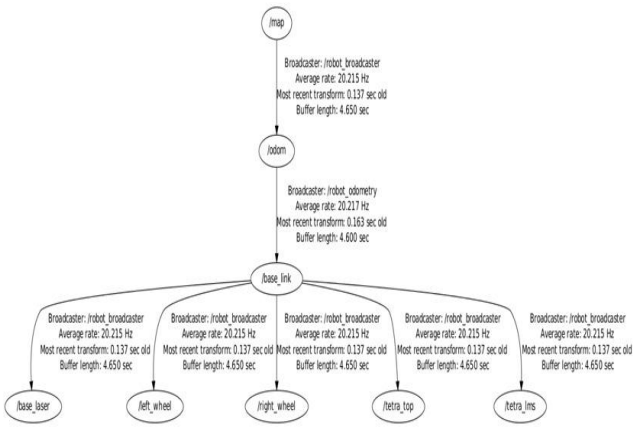

Figure 18 ROS transformation tree frames diagram rqt tf tree

7.3 URDF in Gazebo

The Unified Robotic Description Format (URDF) is an XML file format used in ROS to define all of a robot's components. In order to use a URDF file in Gazebo, some additional simulation-specific tags must be added. This section describes the essential steps to successfully use your URDF-based robot in Gazebo, saving you from having to generate a separate SDF file from scratch and duplicating description formats. Under the hood, Gazebo will then convert the URDF to SDF automatically [36]. The first step to getting your robot working in Gazebo is to have a working URDF file therefore we used the approach of creating a cad design using the Solidworks cad drawing program and then converting the CAD model into URDF format by URDF EXPORTER and then put it in an XML file format. If the URDF is created and suitable as a standard format for Gazebo it will be displayed in Gazebo as shown in figure 19, Therefore, after the transformation of CAD design of URDF file format is handled and set by using the visual studio code program.

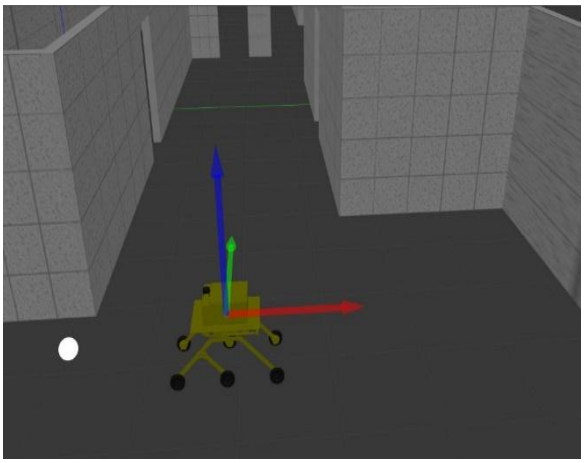

Figure 19 URDF displaying in gazebo world

7.4 Mapping and Navigation

Slam-Gmapping node

Using slam-gmapping, you can create a 2-D occupancy grid map (like a building floorplan) from the laser and pose data collected by a mobile robot. (Light Detection and Ranging), pose data is gained through base-link position, and according to Laser data is obtained from laser scans produced by LIDAR these data the robot can calculate the nearest obstacle position regarding the robot's position, and it draws a map with this given information.

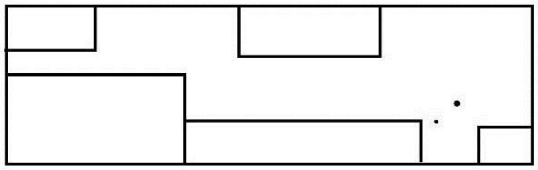

Figure 20 Saved map using the laser scans

AMCL node

Amcl is a probabilistic localization system for a robot moving in 2D. It implements the adaptive Monte Carlo localization approach, which uses a particle filter to track the pose of a robot against a known map [37] According to Monte Carlo's localization principle, the robot assumes many positions with various orientations these samples are filtered to find the correct position with the correct orientation so that the robot can identify its right position.

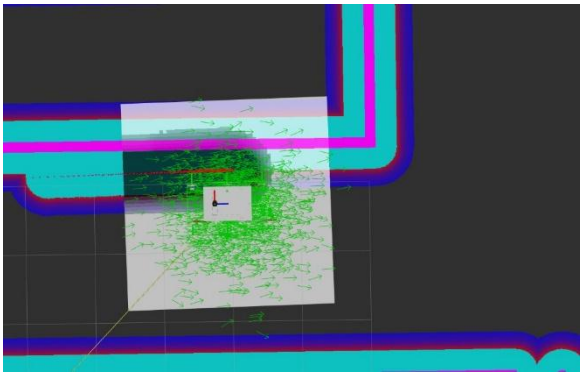

Figure 21 possible assumptions for robot position

Move base node

given a goal in the world, will attempt to reach it with a mobile base. The move-base node links together a global and local planner to accomplish its global navigation task [37]. Where the global planner is the algorithm responsible for making the original path to reach its goal according to the global cost map, while the local planner is responsible for rechecking if this path is still safe if not it redirects the robot to a new safer path furthermore it operates in a local cost map.

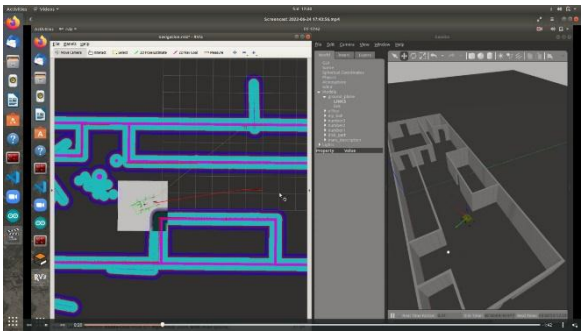

Figure 22 path planned by the robot to reach its goal

Dynamic window Approach (DWA)

The dwa local planner package contains a controller for controlling a mobile base in the plane. This controller is responsible for connecting the path planner to the robot. The planner uses a map to create a kinematic trajectory for the robot to follow from start to finish. Along the way, the planner generates a value function, which is represented as a grid map, at least locally around the robot. The costs of traversing the grid cells are encoded by this value function. The controller's job is to use this value function to determine dx, dy, dtheta velocities to send to the robot.

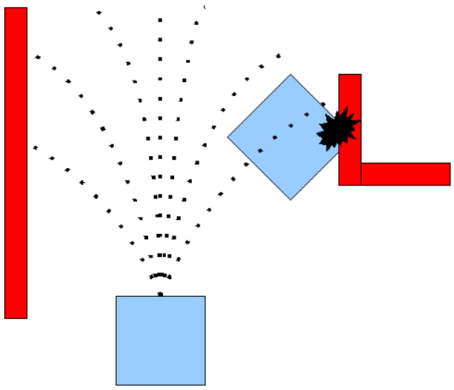

Figure 23 Dynamic Window Approach (DWA) algorithm

8. CONCLUSIONS

This paper presented an autonomous navigation delivery system of the Rocker and Bogie mechanism. The design of the mechanism and component selection, and finite element analysis were summarized. The main advantage of the presented system is its capability to adapt to road segments of different curvatures and the transitions between them. The rocker-bogie mechanism is optimized via the Taguchi method to improve its climbing capability as well as adaptability for various types of stairs. Moreover, to guarantee the stable behavior of the proposed rocker-bogie mechanism during climbing of the stair more rapidly and

efficiently. Finally, the obtained simulation and experimental results show the efficiency of the proposed robot. Future works lie in implementing under ROS more complicated and sophisticated controller methods as well as improving the vehicle's self-localization.

ACKNOWLEDGEMENT

The study was supported by the Canadian International College, 5th Settlement, Cairo, Egypt. The authors express their gratitude to this supportive institute and the supervisor who provided invaluable advice and suggestions to this study.

REFERENCES

[1] S. Fish, UGV's in future combat systems, Proceedings of the SPIE-unmanned Ground Vehicle Technology VI, Orlando, USA, 2004, pp. 288–291.

[2] F.L. Menn, P. Bidaud, F.B. Amar, Generic differential kinematic modeling of articulated multi-monocycle mobile robots, Proceedings of the 2006 IEEE International Conference on Robotics and Automation, Orlando, USA, 2006.

[3] A. Halme, I. Leppanen, J. Soumela, S. Ylonen, I. Kettunen, Workpartner: interactive human-like service robot for outdoor applications, International Journal of Robotics Research 22 (2003) 627–640.

[4] C. Distante, G. Indivery, G. Reina, An application of mobile robotics for olfactory monitoring of hazardous industrial sites, Industrial Robot: An International Journal 36 (2009) 51–59.

[5] R. Volpe, J. Balaram, T. Ohm, R. Ivlev, Rocky7: a next generation Mars rover prototype, Advanced Robotics 11 (1997) 341–358.

[6] R.A. Lindemann, C.J. Voorhees, Mars exploration rover mobility assembly design, test and performance, IEEE International Conference on Systems, Man and Cybernetics, Waikoloa, USA, 2005.

[7] J. Erickson, Living the dream: an overview of the mar's exploration project, IEEE Transactions on Robotics and Automation 13 (2006) 12–18. [8] B. Chen, R. Wang, Y. Jia, L. Guo, L. Yang, Design of a high-performance suspension for lunar rover based on evolution, Acta Astronautica 64 (2009) 925–934.

[9] A. Mechdari, H.N. Pishkenari, A.L. Gaskarimahalle, S.H. Mahboobi, R. Karimi, A novel approach for optimal design of a rover mechanism, Journal of Intelligent and Robotic Systems 44 (2005) 291–312.

[10] K. Nagatani, A. Yamasaki, K. Yoshida, T. Adachi, Development and control method of six-wheel robot with rocker structure, Proceedings of the 2007 IEEE International Workshop on Safety, Security and Rescue Robotics, Rome, Italy, 2007.

[11] W. Chung, G. Kim, M. Kim, Development of the multi-functional indoor service robot PSR systems, Autonomous Robotics 22 (2007) 1–17.

[12] M. Wada, M. Wada, Mechanism and control of a 4WD robotic platform for omnidirectional wheelchairs, Proceedings of the 2009 IEEE/RSJ International Conference on Intelligent Robots and Systems, St. Louis, USA, 2009.

[13] F. Michaud, et al., Multi-modal locomotion robotic platform using leg-track-wheel articulations, Autonomous Robots 18 (2005) 137–156.

[14] D. Chugo, K. Kawabata, H. Kaetsu, H. Asama, T. Mishima, Step climbing omnidirectional mobile robot with passive linkages, Proceedings of SPIEoptomechatronic Systems Control, Sapporo, Japan, 2005.

[15] S. Nakajima, Development of four-wheel-type mobile robot for rough terrain and verification of its fundamental capability of moving on rough terrain, Proceedings of IEEE International Conference on Robotics and Biomimetics, Bangkok, Thailand, 2009.

[16] R. Siegwart, P. Lamon, T. Estier, M. Lauria, R. Piguet, Innovative design for wheeled locomotion in rough terrain, Robotics and Autonomous Systems 20 (2002) 151–162.

[17] S. Nakajima, Concept of a novel four-wheel-type mobile robot for rough terrain, RT-mover, Proceedings of IEEE International Conference on Intelligent Robots and Systems, St. Louis, USA, 2009.

[18] Manash Dey, Harshit Bisht, Rishab Kumar, Abhinav Kumar, Aman Arora, Jatin, "Rocker Rover and Its Implementation in the Field of Agriculture: A Review", Journal of Emerging Technologies and Innovative Research, Volume 6, Issue 6, June 2019.

[19]. Hong-an Yang, Luis Carlos Velasco Rojas*, Changkai Xia, Qiang Guo, School of Mechanical Engineering, Northwestern Polytechnic University, Xi'an, China, Dynamic Rocker-Bogie: A Stability Enhancement for High- Speed Traversal- Vol. 3, No. 3, September 2014, pp. 212~220 ISSN: 2089-4856

[20] P. Panigrahi, A. Barik, Rajneesh R. & R. K. Sahu, "Introduction of Mechanical Gear Type Steering Mechanism to Rocker Bogie", Imperial Journal of Interdisciplinary Research (IJIR) Vol-2, Issue-5, ISSN: 2454-1362,2016.

[21] Fernández, E., Crespo, L. S., Mahtani, A., & Martinez, A. (2015). Learning ROS for robotics programming. Packt Publishing.

[22] M. D. Manik, A. S. Chauhan, S. Chakraborty, V. R. Tiwari, "Experimental Analysis of climbing stairs with the rocker-bogie mechanism", Vol-2 Issue-2 P.No. 957-960IJARIIE-ISSN(O)-2395- 4396, 2016.

[23] Mogg, T. (2018). Startup inks 'world's largest deal' for driverless grocery deliveries. Digital Trends. https://www.digitaltrends.com/cars/autonomous-grocery-delivery-on-its-way-to-oklahoma-city/ Accessed July 1, 2018.

[24] Starship (2017). Starship Technologies launches pilot program with Domino's Pizza Enterprises, https://www.starship.xyz/press_releases/starship-technologies-launches-pilot-program-with-dominos-pizza-enterprises/Accessed July 25, 2018.

[25] Starship (2018). Starship Technologies Launches Commercial Rollout of Autonomous Delivery. https://www.starship.xyz/press_releases/starship-technologies-launches-pilot-program-with-dominos-pizza-enterprises/ Accessed July 1, 2018.

[26] Jennings, D., and Figliozzi, M. (2019). A Study of Road Autonomous Delivery Robots and Their Potential Impacts on Freight Efficiency and Travel, Submitted and presented at Transportation Research Board 99th Annual Meeting. January 2020, Washington DC. Kershner, R. (1939). The number of circles covering a set. American Journal of mathematics, 61(3).

[27] https://www.slamtec.com/en/Lidar/A1

[28] B.K. Rout, R.K. Mittal, Parametric design optimization of 2-DOF R–R planar manipulator—a design of experiment approach, Robotics and ComputerIntegrated Manufacturing 24 (2008) 239–248.

[29] H. Kim, D. Kim, H. Yang, K. Lee, K. Seo, D. Chang, J. Kim, Development of a wall-climbing robot using a tracked wheel mechanism, Journal of Mechanical Science and Technology 22 (2008) 1490–1498.

[30] K. Lee, J. Kim, Controller gain tuning of a simultaneous multi-axis PID control system using the Taguchi method, Control Engineering Practice 8 (2000) 949–958.

[31] G.S. Peace, Taguchi Methods: Hands-on Approach, Addison-Wesley, New York, 1993

[32] S.-H. Baek, S.-H. Hong, S.-S. Cho, D.-Y. Jang and W.-S. Joo, Optimization of process parameters for recycling of mill scale using Taguchi experimental design, Journal of Mechanical Science and Technology, oct 2010, 2127-2134.

[33] H.-K. Kim, J.-Y. Jeon, J.-Y. Park, S. Yoon and S. Na, Noise reduction of a high-speed printing system using optimized gears based on Taguchi's method, Journal of Mechanical Science and Technology, dec 2010 2383-2393.

[34] H. Shin, S. Lee, W. In, J. I. Jeong and J. Kim, Kinematic optimization of a redundantly actuated parallel mechanism for maximizing stiffness and workspace using Taguchi method, Journal of Computational and Nonlinear Dynamics, jan 2011.

[35] R. K. Roy, A primer on the Taguchi method. Society of Manufacturing Engineers, 2010.

[36] Quigley, M., Gerkey, B., & Smart, W. D. (2015). Programming robots with ROS: A practical introduction to the robot operating system. O'Reilly Media.

[37] Fernández, E., Crespo, L. S., Mahtani, A., & Martinez, A. (2015). Learning ROS for robotics programming. Packt Publishing.